JOURNAL OF Applied Polymer SCIENCE

Physical and Thermal Characterization of Polylactic Acid Meltblown Nonwovens

Ryan L. Hammonds, William H. Gazzola, Roberto S. Benson
404 Ferris Hall, Materials Science and Engineering, The University of Tennessee, Knoxville, Tennessee 37996
Correspondence to: R. S. Benson (E-mail: rbenson1@utk.edu)

ABSTRACT: A series of polylactic acid (PLA) nonwovens were prepared by the melt blowing process using micro and nano dies. The nonwovens were characterized for structural, thermal, and mechanical properties. These properties varied with the type of die, airflow, and die to collector distance (DCD). The mean pore size for PLA microfiber ranged between 1.82 and 10.48 micrometers, and nanofiber nonwovens ranged between 452 and 818 nanometers. The tensile modulus and strength of PLA nonwovens increased with airflow at a given DCD, but decreased with increased DCD for a given airflow. Thermograms from calorimetry showed microfiber mats had a larger composition of beta-form crystals than the nanofiber mats. The results showed that a wide range of nonwovens can easily be generated with properties tailored to the specific application. © 2014 Wiley Periodicals, Inc. J. Appl. Polym. Sci. **2014**, *131*, 40593.

KEYWORDS: biomaterials; biopolymers and renewable polymers; fibers; polyesters; textiles

Received 22 August 2013; accepted 11 February 2014
DOI: 10.1002/app.40593

INTRODUCTION

Polylactic acid (PLA) has seen increased interest because it is produced from a renewable source. PLA is a biodegradable aliphatic polyester with physical properties based upon the stereochemical structure and thermal history. This biopolymer can be synthesized by step-growth polymerization using lactic acid monomers or by ring opening polymerization using lactide dimers.[1,2] PLA is used in biomedical engineering as an implant material due to its bioabsorbable and biocompatible properties. PLA degrades via hydrolysis, and the degradation products, namely lactic acid, can be eliminated through the natural human biological processes without adverse effects.

PLA is a thermoplastic polymer that can be processed into a variety of shapes via injection molding, film blowing, or melt spinning. Melt blowing is a process used in commercial production that converts solid polymer directly into a fibrous nonwoven mat. The molten polymer is forced through a number of small diameter holes in a heated die face. Exiting fibers are pushed toward a rotating drum collector with the aid of hot air streams emanating from above and below the die face. The small individual fibers become entangled and form a nonwoven mat. The fibers move in three directions upon exiting the die, where the *z*-direction is toward the collector and movement in the *x* and *y* direction is due to their vibrational motion. The vibrational motion within 1 cm of the die exit is responsible for fiber entanglement.[3] In addition, hot air streams at the die exit attenuate the fibers as they travel toward the collector. The fibers are accelerated and reach a maximum velocity of 40–70 m/s around 8–10 cm away from the die.[4] At this point, the stress generated in the fibers by their rapid acceleration goes to zero, with the maximum stress occurring in the fibers about 2 cm from the die.[4] The fiber temperature decreases drastically within the first 5 cm away from the face of the die.[5]

The melting temperature of PLA is 207°C, but decreases to between 170 and 180°C in high molecular weight PLA due to the presence of enantiomeric and other impurities causing imperfect crystals and lower melt temperatures. Still, PLA must be processed at high temperature in an inert environment. Studies have shown that in air, PLA undergoes thermo-oxidative degradation by a single stage process that produces a lactide decomposition product. PLA begins to degrade in air at temperatures as low as 70°C.[6] Drying of the pellets is required before processing. Studies have shown that even with low levels of moisture, at a concentration of approximately 50 ppm, the degradation rate increases during extrusion and allowable residence time decreases.[7] Researchers have found that under an inert atmosphere, PLA can resist significant volatilization during heating up to approximately 250°C.[8] Isothermal weight loss studies have shown that in a N_2 gas environment, PLA has a small processing window above its melting temperature where little to no weight loss occurs over a 30-min time period.[9] Accompanying increases in temperature are changes in viscoelastic properties of PLA. The melt flow rate (MFR) of PLA increases from 4.2 cm^3 per 10 min at 150°C to 8.6 cm^3 per 10 min at 200°C.[8] Studies have shown that PLA exhibits

Newtonian behavior up to a shear rate of 10 rads/s,[10,11] but will exhibit shear thinning behavior as the shear rate increases to 1000 rad/s.[12]

The thermal history of polymers affects the physical properties as a consequence of the crystal type and quantity formed. PLA has three crystalline morphologies α, β, and γ.[13] The α-form has a 10_3 helix conformation and grows from the melt or during cold crystallization. The β-form has a left-handed 3_1 helix conformation and grows under non-isothermal cooling as frustrated crystallization or under high draw ratio. The γ-form crystals are observed during epitaxial crystallization.

The goal of this study is to investigate the effects of airflow and die to collector distance (DCD) on the physical and thermal properties including cold crystallization, melting temperature, fiber diameter, pore size, tensile modulus, and tensile strength of the generated PLA nonwovens. Thus, the purpose is to gain fundamental understanding of the processing parameters required to tailor the properties of PLA nonwovens to meet specific requirements for tissue scaffolds. Unique to this study is the generation of PLA nonwovens with micro and nanofibers.

EXPERIMENTAL

Materials

The PLA used in this study was Inego™ biopolymer 6252D, purchased from NatureWorks® (Minnetonka, MN). Before processing, the PLA pellets were dried at 80°C for 4 h under vacuum to remove moisture.

Molecular Weight Determination

The viscosity-average molecular weight, M_v was determined using a Ubbelohde viscometer (Cannon Instruments, State College, PA). Five PLA-chloroform solutions of different concentrations were made for testing. The Ubbelohde viscometer and polymer solution was placed in a water bath at 25°C and allowed to equilibrate before acquiring data. The Mark-Houwink-Sakurada relationship was used to determine viscosity-average molecular weight, M_v. The K and a values used for PLA in chloroform were 5.45×10^{-4} and 0.73, respectively.[14]

Melt Blowing of PLA Nonwovens

The processing was performed without the aid of additives or stabilizers. Extrusion of the PLA was performed using a twin-screw extruder (Haake, Saddle Brook, NJ) under N_2 gas flow in order to prevent thermo-oxidative degradation of the polymer during processing. Melt blowing was conducted on a 15.24 cm (6 in.) line using micro (ExxonMobil, Irving, TX) and nano (Arthur G. Russell Co., Bristol, CT) dies in the process. Nonwoven samples were collected on a rotating drum (12 and 3 m/min) at a constant basis weight of 20 g/m^2. The nonwoven samples were produced by varying airflow between 1 and 35 m^3/min and varying DCD distances at 0.10, 0.30, and 0.50 m. A summary of the die properties and processing parameters is presented in Table I.

The structural properties (fiber diameter and porosity), mechanical (modulus and tensile strength), and thermal of the meltblown PLA nonwovens were determined by selecting random sections from along the centerline of nonwoven mats.

Table I. Die Properties and Processing Parameters

Die properties	Micro die	Nano die
Hole diameter (μm)	254	25.4
Holes per inch	20	100
Throughput (g/hole/min)	0.3	0.025
Die angle (degrees)	30	-
Die set back (mm)	2.032	-
Die air gap (mm)	1.52	-
Processing parameters	Micro die	Nano die
Extruder zone 1 (°C)	162	164
Extruder zone 2 (°C)	210	215
Extruder/die connector (°C)	225	230
Top die face (°C)	220	242
Bottom die face (°C)	220	244
Extruder screw speed (RPM)	30	20
Metering pump speed (RPM)	30	6
Collector speed (m/min)	12	3

Presented in the table are properties and parameters used for the "ExxonMobil" micron hole size die and "AGR" nano hole size die.

Thermal Gravimetric Analysis

Thermogravimetric analysis (TGA) was performed on dried PLA pellets under the flow of N_2 gas (40 cc/min) on a Mettler Toledo Star System TGA (Columbus, OH). Samples were heated from 25 to 600°C at a rate of 10°C/min.

Fiber Diameter Measurements

Before fiber size analysis, the PLA nonwoven samples were mounted on aluminum studs using carbon tape and coated for 20 s with gold in an argon environment at 20 milliamps. A Leo1525 scanning electron microscope (SEM) equipped with Zeiss SmartSEM software was used to collect images of each nonwoven for fiber diameter measurements. Four areas from each meltblown nonwoven were sampled to acquire more than 94 fiber diameter measurements for each nonwoven. ImageJ version 1.45s (Wayne Rasband National Institute of Health, USA) was used to obtain measurements of fiber diameter from the SEM images. JMP® Pro 10.0.0 software (SAS Institute, Cary, NC) was used to determine the mean fiber diameter and distribution for each web.

Pore Size Determination

Pore sizes for each PLA nonwoven were determined using a Capillary Flow Porometer, Model CFP-1100-AEX (Porous Materials, Ithaca, NY). Samples from three areas of the nonwoven were selected and tested for porosity. Data analysis was performed using JMP software.

Tensile Testing

Tensile testing was performed according to ASTM D5035-06 to determine the tensile modulus and strength of PLA nonwovens in the machine (MD) and transverse direction (TD). Samples for testing were 12.7 cm by 2.54 cm. Eight samples in the

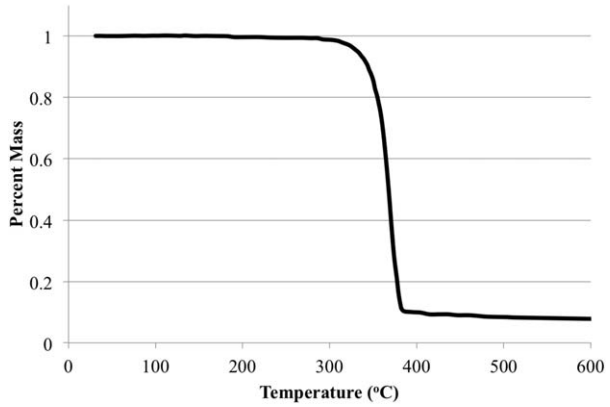

Figure 1. PLA TGA mass loss curve. Presented here is the percent mass loss of PLA as the temperature is increased.

transverse direction and five in the MD were used to determine these properties. A United Model SSTM-1-E-PC Tensile Testing machine equipped with a 4.5 kg load cell (±1% precision) was used to conduct the tests at a crosshead speed of 30.48 cm/min. Each PLA nonwoven sample started with an initial gauge length of 7.6 cm and was tested until failure.

Differential Scanning Calorimetry

The differential scanning calorimetry (DSC) was conducted using a Mettler Toledo Star System DSC 822e according to ASTM D3418-08. This technique was used to follow the melting behavior of PLA nonwovens as a function of processing parameters. A 5–10 mg sample was obtained from each meltblown nonwoven web, placed in an aluminum DSC pan, and heated from 30 to 200°C at 10°C/min. The sample was allowed to equilibrate at 200°C for 2 min before being cooled back to room temperature at 5°C/min. All DSC experiments were conducted using a N_2 environment at 200 cc/min.

RESULTS AND DISCUSSION

Molecular Weight Determination

Five measurements of flow time were recorded at each solution concentration of PLA in chloroform through the Ubbelohde viscometer. A Huggins-Kraemer plot was used to calculate the M_v of PLA. The calculated M_v from the measurement of intrinsic viscosity was 35,485 g/mol.

Thermogravimetric Analysis

The mass loss versus temperature curve for NatureWorks 6252D PLA was over the thermal range of 25–600°C and presented in Figure 1. The degradation process for PLA begins at approximately 300°C, proceeds rapidly, and nears completion of mass loss at 375°C with 7.8% of the original mass remaining as char. This data agrees with studies conducted by other researchers on PLA.[8,9] After processing, no degradation was expected or detected in the meltblown nonwovens since the die face temperatures in this study were 220 and 244°C for the microdie and nanodie, respectively. In addition, studies have shown that PLA has a processing temperature window of 30 min during thermal treatment up to 250°C.[8] The die temperature used in this study was below the initial degradation temperature of 250°C.

Fiber Size Distributions

The fiber size is a critical parameter that must be controlled to enable tailoring of scaffolds for cell growth, as fiber diameter has been shown to effect cell adhesion and spreading.[15] The mean fiber diameters for PLA microfiber and nanofiber nonwovens are presented in Figure 2. The microfibers were reduced down to as much as 0.7% of their original 254 μm diameter at the die exit while the nanofibers were reduced down to as much as 2% of their original 25.4 μm diameter. There is a substantial decrease in microfiber diameter with increase in airflow. The microfiber diameter decreases one order of magnitude over an airflow increase from 0.8 m^3/min to 35 m^3/min and does so in a linear manner with a correlation factor (R^2) of 0.93. The confidence interval also decreases with increasing airflow. Fiber diameter reduction can be attributed to parallel forces from the effective airflow attenuating the fibers. These results are supported by microfiber nonwovens produced by other researchers.[3,14] Figure 2(A) also shows that fiber diameter is not affected by the DCD in a statistically significant manner.

The dependence of fiber diameter on airflow and DCD for nanofibers in PLA nonwovens show fiber diameters relatively independent of airflow with a dependence on DCD. This trend is contrary to that observed for the microfiber nonwovens. The

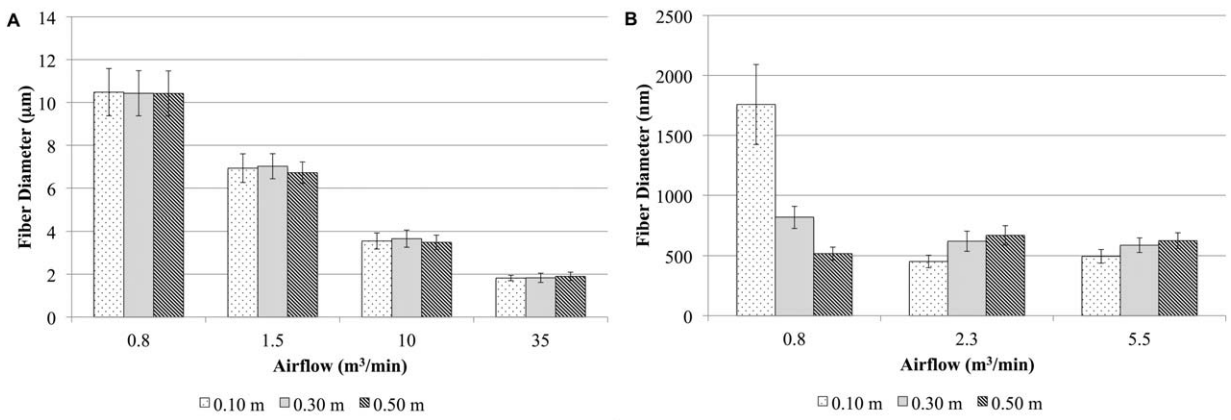

Figure 2. Fiber diameter versus processing parameters. Averages and 95% confidence intervals are presented versus airflow and DCD. PLA microfiber nonwoven (A) and meltblown PLA nanofiber nonwoven (B) are presented.

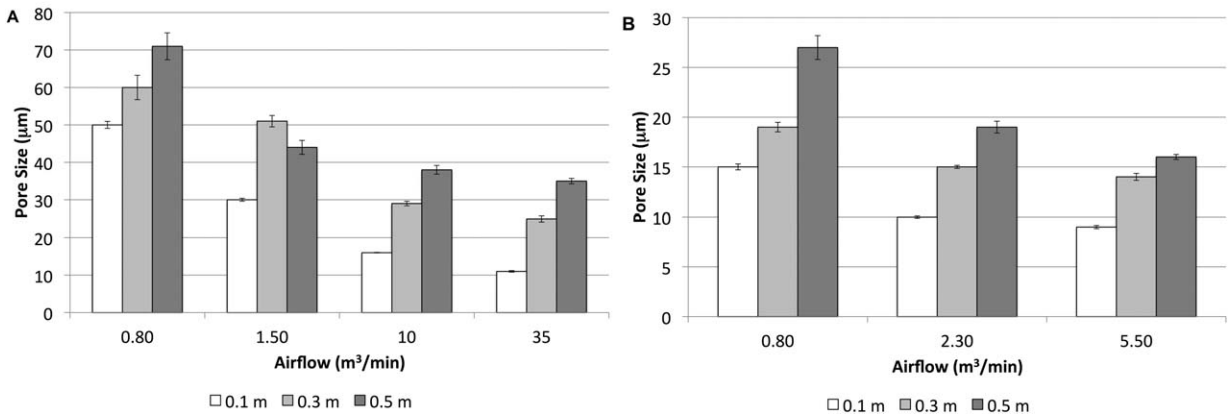

Figure 3. Pore size versus processing parameters. Averages and 95% confidence intervals are presented versus airflow and DCD. PLA microfiber nonwoven (A) and meltblown PLA nanofiber nonwoven (B) are presented.

diameters of nanofibers processed at low airflow (0.8 m^3/min) and collected at all DCD show some discrepancy with respect to other airflow values. At present, the origin of this disparity is not well understood. Significant reductions from the original die size to final fiber diameters were measured.

The rapid cooling and fiber–fiber interactions are responsible for the lack of strong correlation between fiber diameter and processing parameters for the nanodie. Researchers have shown that in general the fibers produced via melt blowing often do not solidify until they are laid down on the collector.[16] Therefore, it is possible for the diameter of the fibers to change throughout their journey from DCD. As the majority of the stress imposed on the fibers occurs 2–4 cm from the die, the majority of fiber attenuation occurs in that region. However, it has been observed that fiber diameter continues to change, albeit minimally, at large distances away from the die.[15] The current consensus is that fiber attenuation occurs due to aerodynamic drag during the melt blowing process.[17] Fiber diameter may increase during melt blowing by fiber–fiber fusion and disorientation upon impact of the collector. These two factors could be responsible for the lack of correlation.

In small diameter fibers, such as those in the nanofiber mats, the rapid evolution of heat prevents continuous fiber attenuation and reduction in the diameter. The smaller diameter fibers emanating from the nanodie are able to cool much faster, and thus preclude further reduction in diameter. This, in part, may account for the discrepancy observed at short collection distances. Still, all fibers produced using the nanodie die have a similar diameter and are smaller than those produced using the microdie.

Pore Size Distributions

Similar to fiber size, studies have shown a dependence on cells traversing through the nonwoven as a pore size dependent behavior.[17] The mean pore sizes of PLA nonwovens using the microdie and nanodie are presented in Figure 3 to illustrate the effects of processing conditions. The general trend for both PLA microfiber and nanofiber nonwovens is a decrease in the pore size with increasing airflow. Also, as the DCD increases, so does the mean pore size for each airflow. The PLA microfiber nonwovens had a larger mean pore size than PLA nanofiber nonwovens. While the effect of airflow in PLA nanofiber nonwovens was similar to that observed for the microfiber PLA nonwovens, the overall effect was much smaller when compared to the microfiber nonwovens. Increasing the airflow by 1 m^3/min for the meltblown microfiber nonwovens caused a decrease of 20 to 30 μm. Further increasing the airflow by 5 m^3/min only caused a mean pore size decrease of about 5 to 10 μm at the same DCD. For nanofiber nonwovens, an increase in airflow of 1 m^3/min produced a much smaller decrease in pore size of approximately 4 μm.

The mean pore size decreases with an increase in airflow as expected since an increase in the airflow causes a decrease in fiber diameter of the microfiber nonwovens. A decreased fiber diameter results in longer collection times in order to attain the desired basis weight (20 g/cm^2). The collector speed decreases and collection time increases, allowing more fibers to be laid down in the same unit area and producing random fiber overlapping with mean pore size decreasing.

Since the diameter for the nanofibers did not vary significantly with airflow, the decrease in pore size cannot be directly associated with fiber diameter. Here the decrease in pore size with airflow is due to extended time required to attain the desired basis weight. The rate of fiber accumulation is much slower (3 m/min) for PLA nanofiber nonwovens due to the smaller mass per fiber collected compared to the micro-webs. The smaller fibers resulted in more time for the nonwoven thickness to increase and subsequently collapse the nonwoven structure leading to a decreased pore size.

As DCD increased, the mean pore size increased for all airflow rates for microfiber and nanofiber nonwovens. The fibers possess velocity in three-dimension, so an increase in the collection distance causes an increase in the area over which the fibers are laid down. These results indicate that mean pore size of a PLA tissue scaffold can be controlled to allow for nutrients and cell infiltration. In addition, the presence of pores also allows for the removal of cellular waste.

Mechanical Properties

The stiffness of cell scaffolds and substrates is critical as it directly affects cell interactions and gene expression in

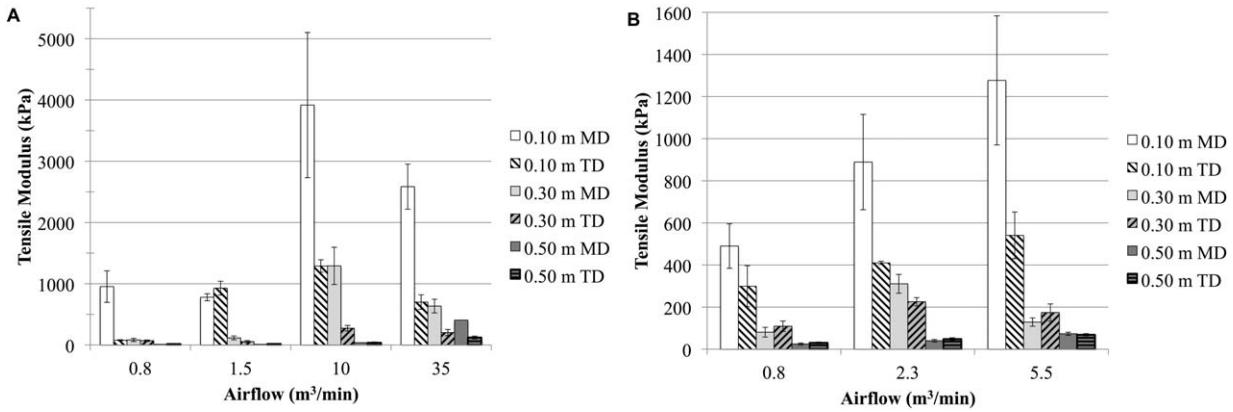

Figure 4. Tensile modulus versus processing parameters. Averages and 95% confidence intervals are presented versus airflow and DCD. PLA microfiber nonwoven (A) and meltblown PLA nanofiber nonwoven (B) are presented.

mesenchymal stem cells.[16] The tensile modulus in MD and TD for PLA microfiber and nanofiber nonwovens are shown in Figure 4. Microfiber mats exhibited a significant decrease in tensile modulus (MD and TD) as the DCD increased from 0.10 m to 0.50 m. The tensile modulus showed a smooth dependence on DCD and decreased for both MD and TDs with increasing DCD for nearly all samples. The tensile modulus has a maximum at airflow of 10 m^3/min for the PLA microfiber nonwovens. Nanofiber mats exhibited a smooth, consistent trend of increasing moduli with increased airflow and decreasing moduli with increased DCD. PLA nanofiber nonwovens exhibited an increase in MD and TD with increased airflow.

The effect of airflow and DCD on the tensile strength of the microfiber and nanofiber nonwovens is presented in Figure 5. The tensile strength of the microfiber and nanofiber nonwovens increased with airflow, but decreased with DCD for a given airflow. The change in tensile strength of PLA microfiber nonwovens is smooth and attains higher values due to larger fiber diameters. The effect of DCD for PLA microfiber nonwovens was minimal at low airflow. At larger DCD, an increase in airflow caused a small increase in tensile strength. The PLA nanofiber nonwovens also showed tensile strength increased moderately with increasing airflow. PLA microfiber and nanofiber nonwoven tensile strength generally decreased in MD and TD with increased in DCD.

The tensile strength of the nonwovens show similar results with decreases in strength with increased DCD and airflow. The tensile strengths of PLA microfiber nonwovens are nominally higher than PLA nanofiber nonwovens due to larger fiber diameters.

The disparity in tensile modulus and strength between MD and TD is due to preferential direction of fibers leaving the die during melt blowing. Studies have shown that fibers in meltblown nonwovens have a slight preference for the MD compared to the TD.[12] The increase in tensile strength for PLA microfiber and nanofiber nonwovens with airflow is also explained by the fiber orientation. At greater airflow, the fibers have a greater tendency to produce anisotropic mats by preferentially aligning with the MD and produce stronger mats in the MD and weaker mats in the TD. The fiber alignment decreases with increased DCD since the airflow at the collector decreases.[3] In addition, molecular orientation can be imparted to the fiber during its travel to the collector. An explanation for this preferred orientation is the airflow toward the collector assists in drawing fibers. At shorter DCD, the fibers are cooled rapidly as they collect on the target and trap the drawn fiber morphology. As the DCD is increased, the polymer chains have more time to assume a more relaxed state with less molecular alignment. Greater DCD

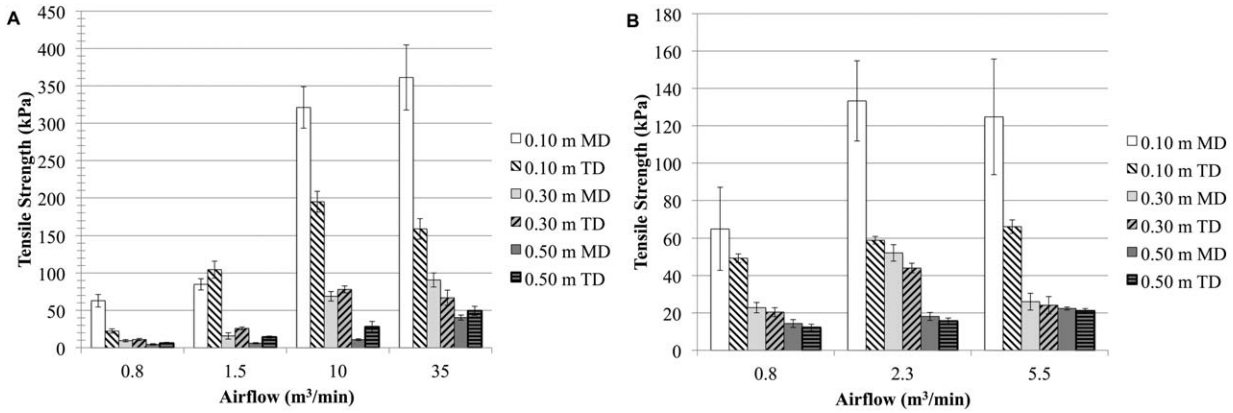

Figure 5. Tensile strength versus processing parameters. Averages and 95% confidence intervals are presented versus airflow and DCD. PLA microfiber nonwoven (A) and meltblown PLA nanofiber nonwoven (B) are presented.

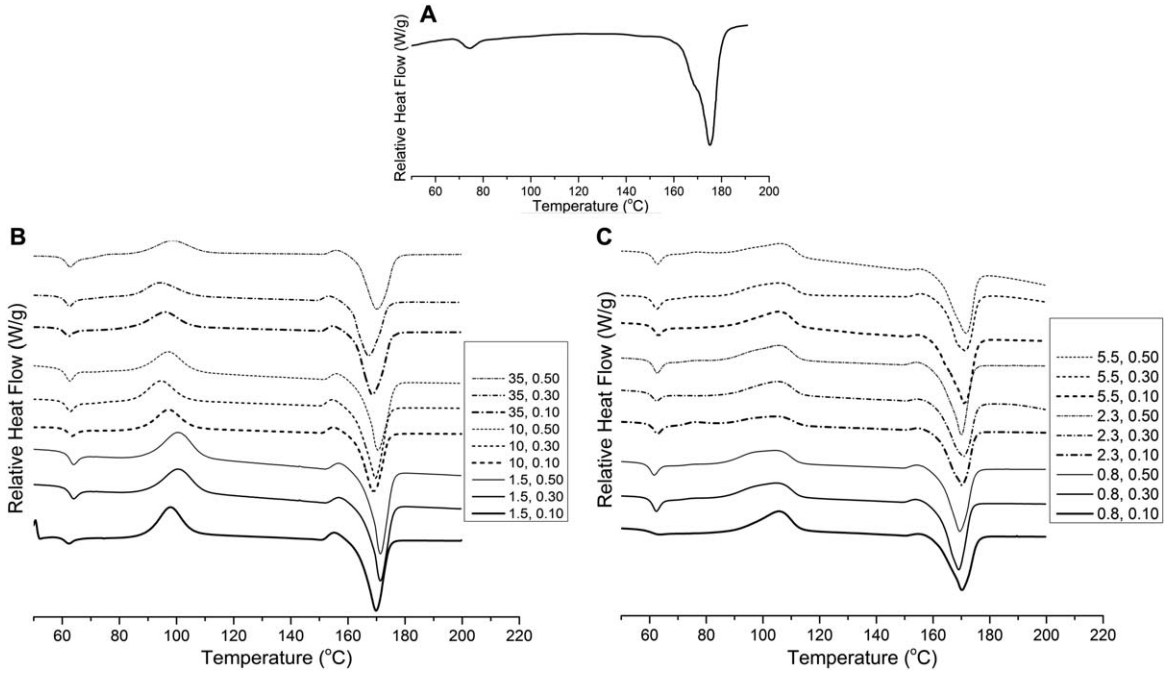

Figure 6. Thermal properties versus processing parameters. DSC thermograms of PLA as-received (A), microfiber nonwovens (B) and nanofiber nonwovens (C) are shown. The legend in each plot identifies the processing airflow (m^3/min) followed by the DCD (m).

results in nonwovens with less orientation and isotropic mechanical properties. This tendency is noticeable at 0.50 m DCD.

Differential Scanning Calorimetry (DSC)

The DSC thermograms for as-received PLA and meltblown PLA microfiber and nanofiber nonwovens are presented in Figure 6. The DSC thermogram for the as-received PLA exhibits a glass transition temperature (T_g) at 74°C and a melting temperature (T_m) at 170°C. On the other hand, thermograms for PLA microfiber and nanofiber nonwovens exhibit four distinct features: an endothermic peak associated with the glass transition temperature at 62°C, an exothermic peak near 100°C associated with cold crystallization leading to formation of α crystals, another exothermic peak near 155°C associated with crystal phase transition, and an endothermic peak with the onset of melting near 160°C with the peak melting temperature near 170°C. The major difference between the as-received PLA and meltblown PLA nonwoven thermograms is the presence of an exothermic (cold crystallization) peak around 100°C. There is a slight difference in the position and width of this exothermic peak corresponding to the cold crystallization of PLA microfiber and nanofiber nonwoven samples. The cold crystallization process occurs over a slightly wider temperature range for the nanofiber nonwovens. The cold crystallization peak in the microfiber nonwovens shifts to higher temperature with increased DCD. The cold crystallization peaks broaden and become asymmetric with increase in DCD for nanofiber nonwovens.

The glass transition temperature in the PLA nonwoven fibers is at a lower temperature (62°C) than observed for the as-received sample, indicating a lower energy barrier to attain chain flexibility in the amorphous phase of the nonwoven microfibers and nanofibers. The exothermic peak associated with cold crystallization is present in all DSC thermograms of PLA microfiber and nanofiber nonwovens. PLA is a slow crystallizer with the half life for pure PLA crystallization taking 17–45 min.[18] Melt blowing is a process where non-isothermal crystallization takes place as the fiber travels from the hot die to the room temperature collector. This process results in non-isothermal crystallization and an expected retardation of crystal formations due to rapidly cooling fibers and reduces the polymer chain motions necessary for the crystallization process. In addition, the shear flow contributes to retardation of the onset cold crystallization.[19] As the PLA nonwovens are heated above the T_g, chains acquire the freedom to move and are able to crystallize. As a result, the exothermic peaks seen just below 100°C can be explained as cold crystallization exotherms.[18] The thermal range for PLA microfiber nonwoven mats is symmetrical and covers a range of 82–110°C. The width of the cold crystallization peak is asymmetric and wider in the case of the nanofiber mats, 82–117°C. These discrepancies in thermal ranges observed for cold crystallization of PLA microfibers and nanofibers indicate differences in the chain microenvironments in the interior of the fiber. Chains subjected to higher orientation in the amorphous phase would require higher energy input to acquire the mobility necessary for crystallization to ensue.

The presence of the peak at 155°C is attributed to crystal transition from a less ordered β form having 3_1 helical conformation to more ordered α form with a 10_3 helical conformation. The presence of the less organized crystal structure in the interior of the fiber can be explained as polymer flow during the processing resulting in radial distribution of crystal perfection.[20] This is reflected in increases of the onset of cold crystallization for microfibers. The polymer flow through the die can effect the

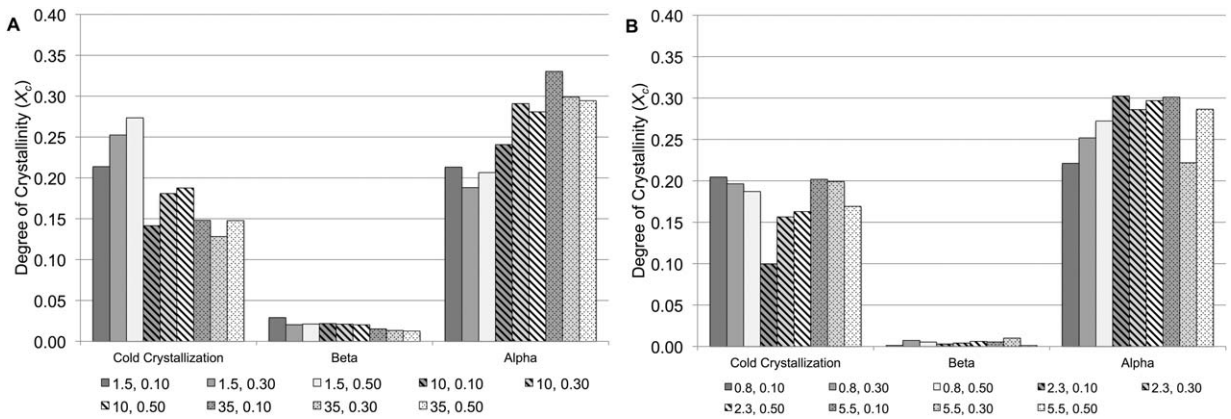

Figure 7. Crystallinity versus processing parameters. The degree of crystallinity of PLA meltblown microfiber (A) and nanofiber nonwovens (B) are presented with respect to the cold crystallization contribution as well as degree of crystallinity values from α-form and β-form crystals. The legend in each plot identifies the processing airflow (m^3/min) followed by the DCD (m).

internal microstructure of the fiber.[20] Differences in the interior fiber microstructure are more prevalent for the larger microfibers than for the nanofibers. This is indicated by a higher presence by of β crystals from the DSC thermograms in Figure 6 and quantified in Figure 7. The larger mass of microfibers produces a different cooling rate than the nanofibers experience and results in the production of different crystal structures. Since the degree of crystallinity of these nonwovens is low, an annealing step can be used to further increase the crystallinity and improve their mechanical properties.[18]

Figure 7 shows the crystallinity from α and β-form crystals along with cold crystallization for PLA microfiber and nanofiber mats. The cold crystallization peak reduces with airflow for microfibers. The same cannot be said of nanofiber mats. Another significant trend is the greater content of β crystals in microfiber mats versus nanofiber mats. Otherwise, the α crystal content in microfiber mats roughly increases with airflow and remains relatively independent for nanofiber mats.

CONCLUSIONS

Polylactic acid nonwovens were successfully formed under appropriate processing conditions using a microdie and a nanodie. The properties of these nonwovens were dependent on the processing parameters such as die hole diameter, airflow, and DCD. The data trends between processing parameters and die size are similar for pore size, tensile modulus, and tensile strength, but different for fiber diameter. The overall mean pore size and air permeability for PLA microfiber and nanofiber nonwovens decreased with airflow, but increased with DCD. The tensile strength of PLA nonwovens increased with airflow at a specific distance, but decreased with increased DCD for a given airflow.

REFERENCES

1. Kim, S. H.; Kim, Y. H. *Macromol. Symp.* **1999**, *144*, 277.
2. Cheng, M.; Attygalle, A. B.; Lobkovsky, E. B.; Coates, G. W. *J. Am. Chem. Soc.* **1999**, *121*, 11583.
3. Bresee, R. R.; Qureshi, U. A. *Int. Nonwovens J.* **2003**, *8*, 49.
4. Marla, V. T.; Shambaugh, R. L. *Ind. Eng. Chem. Res.* **2003**, *42*, 6993.
5. Zhao, R.; Wadsworth, L. C. *J. Appl. Polym. Sci.* **2003**, *89*, 1145.
6. Gupta, M. C.; Deshmukh, V. G. *Colloid Polym. Sci.* **1982**, *260*, 308.
7. Wang, Y. M.; Steinhoff, B.; Brinkmann, C.; Alig, I. *Polymer* **2008**, *49*, 1257.
8. Nalbandi, A. *Iranian Polym. J.* **2001**, *10*, 371.
9. Signori, F.; Coltelli, M.-B.; Bronco, S. *Polym. Degrad. Stab.* **2009**, *94*, 74.
10. Corre, Y.-M.; Maazouz, A.; Duchet, J.; Reignier, J. *J. Supercrit. Fluids.* **2011**, *58*, 177.
11. Shin, B. Y.; Cho, B. H.; Hong, K. H.; Kim, B. S. *Polymer-Korea* **2009**, *33*, 588.
12. Palade, L. I.; Lehermeier, H. J.; Dorgan, J. R. *Macromolecules* **2001**, *34*, 1384.
13. Zhang, J. M.; Duan, Y. X.; Sato, H.; Tsuji, H.; Noda, I.; Yan, S.; Ozaki, Y. *Macromolecules* **2005**, *38*, 8012.
14. Badami, A. S.; Kreke, M. R.; Thompson, M. S.; Riffle, J. S.; Goldstein, A. S. *Biomaterials* **2006**, *27*, 596.
15. Bresee, R. R.; Qureshi, U. A. *J. Eng. Fiber Fabric.* **2006**, *1*, 32.
16. Peyton, S. R.; Kalcioglu, Z. I.; Cohen, J. C.; Runkle, A. P.; Van Vliet, K. J.; Lauffenburger, D. A.; Griffith, L. G. *Biotechnol. Bioeng.* **2011**, *108*, 1181.
17. Kim, I. L.; Khetan, S.; Baker, B. M.; Chen, C. S.; Burdick, J. A. *Biomaterials* **2013**, *34*, 5571.
18. Harris, A. M.; Lee, E. C. *J. Appl. Polym. Sci.* **2008**, *107*, 2246.
19. Li, X. J.; Zhong, G. J.; Li, Z. M. *Chin. J. Polym. Sci.* **2010**, *28*, 357.
20. Xin, S. F.; Wang, X. H. *Polym. Eng. Sci.* **2012**, *52*, 1325.